CHEMISTRY
A EUROPEAN JOURNAL

DOI: 10.1002/chem.200701281

Hydration of Lanthanoid(III) Ions in Aqueous Solution and Crystalline Hydrates Studied by EXAFS Spectroscopy and Crystallography: The Myth of the "Gadolinium Break"

Ingmar Persson,*[a] Paola D'Angelo,[b] Simone De Panfilis,[c] Magnus Sandström,[d] and Lars Eriksson[d]

Abstract: The structures of the hydrated lanthanoid(III) ions including lanthanum(III) have been characterized in aqueous solution and in the solid trifluoromethanesulfonate salts by extended X-ray absorption fine structure (EXAFS) spectroscopy. At ambient temperature the water oxygen atoms appear as a tricapped trigonal prism around the lanthanoid(III) ions in the solid nonaaqualanthanoid(III) trifluoromethanesulfonates. Water deficiency in the capping positions for the smallest ions starts at Ho and increases with increasing atomic number in the $[Ln(H_2O)_{9-x}](CF_3SO_3)_3$ compounds with $x=0.8$ at Lu. The crystal structures of $[Ho(H_2O)_{8.91}](CF_3SO_3)_3$ and $[Lu(H_2O)_{8.2}](CF_3SO_3)_3$ were re-determined by X-ray crystallography at room temperature, and the latter also at 100 K after a phase-transition at about 190 K. The very similar Ln K- and L_3-edge EXAFS spectra of each solid compound and its aqueous solution indicate indistinguishable structures of the hydrated lanthanoid(III) ions in aqueous solution and in the hydrated trifluoromethanesulfonate salt. The mean Ln–O bond lengths obtained from the EXAFS spectra for the largest ions, La–Nd, agree with estimates from the tabulated ionic radii for ninefold coordination but become shorter than expected starting at samarium. The deviation increases gradually with increasing atomic number, reaches the mean Ln–O bond length expected for eightfold coordination at Ho, and increases further for the smallest lanthanoid(III) ions, Er–Lu, which have an increasing water deficit. The low-temperature crystal structure of $[Lu(H_2O)_{8.2}](CF_3SO_3)_3$ shows one strongly bound capping water molecule (Lu–O 2.395(4) Å) and two more distant capping sites corresponding to Lu–O at 2.56(1) Å, with occupancy factors of 0.58(1) and 0.59(1). There is no indication of a sudden change in hydration number, as proposed in the "gadolinium break" hypothesis.

Keywords: EXAFS spectroscopy · hydrates · lanthanides · solution structures · X-ray diffraction

Introduction

In the lanthanoid series of fifteen chemically similar elements including lanthanum, systematic changes in their chemical properties take place. At an early stage the series was divided into two subgroups, the light and heavy lanthanoids.[1] However, the point of division depended on the observed property and was somewhat indefinite until Spedding and co-workers some 40 years ago proposed the so-called gadolinium break. This concept was based on changes in a number of physicochemical properties, such as partial molar volume,[2] heat capacity,[3] molar entropy[3] and viscosity[4] around samarium, europium, and gadolinium, and assumed to be related to the half-filled 4f shell of gadolinium(III). The partial molar volumes should decrease continuously taking the lanthanoid contraction into account if the hydrated lanthanoid(III) ions have the same hydration structure.

[a] Prof. I. Persson
Department of Chemistry
Swedish University of Agricultural Sciences
P.O. Box 7015, 75007 Uppsala (Sweden)
Fax: (+46) 1867-3392
E-mail: Ingmar.Persson@kemi.slu.se

[b] Prof. P. D'Angelo
Dipartimento di Chimica, Università di Roma "La Sapienza"
Piazzale de Aldo Moro 5, 00185 Roma (Italy)

[c] Dr. S. De Panfilis
CRS-SOFT INFM-CNR, Dipartimento di Fisica, Università di Roma "La Sapienza"
Piazzale de Aldo Moro 5, 00185 Roma (Italy)

[d] Prof. M. Sandström, Dr. L. Eriksson
Department of Physical, Inorganic and Structural Chemistry
Stockholm University, 10691 Stockholm (Sweden)

Supporting Information for this article is available on the WWW under http://www.chemeurj.org/ or from the corresponding author.

Table 1. Summary of Ln–O bond lengths in $[Ln(H_2O)_9](CF_3SO_3)_3$, $[Ln(H_2O)_9](C_2H_5SO_4)_3$, $[Ln(H_2O)_n]I_3$ [$n=9$ for La–Ho and $n=8$ for Er and Lu (values in bold)], $[Ln(H_2O)_9](BrO_3)_3$, and $[Ln(H_2O)_8]Br_3$ (values in bold).

Ln	$[Ln(H_2O)_9](CF_3SO_3)_3$[a] $Ln-O_p+Ln-O_c$/mean	$[Ln(H_2O)_9](C_2H_5SO_4)_3$[b] $Ln-O_p+Ln-O_c$/mean	$[Ln(H_2O)_n]I_3$[c] Ln–O range/mean	$[Ln(H_2O)_9](BrO_3)_3$[d] $Ln-O_p+Ln-O_c$/mean	$[Ln(H_2O)_8]Br_3$[e] Ln–O range/mean	$[Ln(H_2O)_n]^{3+}$[f] Ln–O mean
La	2.515+2.614/2.548	2.517+2.615/2.550	2.538–2.572/2.549			2.542
Ce	2.491+2.594/2.525	2.491+2.600/2.527				2.538
Pr	2.470+2.579/2.506	2.470+2.587/2.509	2.520–2.541/2.526	2.489+2.521/2.500		2.503
Nd	2.451+2.568/2.490	2.458+2.570/2.495	2.507–2.519/2.512			2.488
Sm	2.422+2.549/2.464	2.430+2.550/2.470	2.445–2.487/2.461	2.462+2.550/2.491		2.455
Eu	2.408+2.536/2.452	2.416+2.542/2.458				2.424
Gd	2.397+2.538/2.444	2.401+2.537/2.446	2.423–2.458/2.438			2.415
Tb	2.380+2.527/2.429	2.382+2.526/2.430		2.405+2.469/2.426		2.390
Dy	2.364+2.520/2.416	2.371+2.517/2.420				2.373
Ho	2.353+2.527/2.411[f]	2.362+2.511/2.412	2.400–2.420/2.404	2.382+2.446/2.404	**2.329–2.429/2.369**	2.359
Er	2.340+2.518/2.399[g]	2.357+2.514/2.409	**2.315–2.366/2.336**			2.350
Tm	2.322+2.522/2.386[g]	2.340+2.504/2.395				2.334
Yb	2.303+2.538/2.376[g]	2.323+2.511/2.386		2.321+2.431/2.358		2.317
Lu	2.288+2.510/2.359[g]	2.318+2.497/2.378	**2.291–2.340/2.303**		**2.288–2.391/2.319**	2.310

[a] Refs. [19–23]. [b] Refs. [24–26]. [c] Refs. [31–34]. [d] Refs. [27–30]. [e] Refs. [34,35]. [e] Ref. [17]. [f] This work. [g] Water deficit in the complex.[23]

However, there is a discontinuity, with an increase in the partial molar volumes from samarium to gadolinium, which was rationalized by an assumed decrease in the hydration number of the heavy lanthanoid(III) ions.[2] The hydrated light lanthanoid(III) ions were shown to be nine-coordinate in aqueous solution, consistent with a tricapped trigonal-prismatic configuration, while the heavy ones were proposed to coordinate eight water molecules in a square antiprism.[5–7] The water exchange rates decrease, as expected, with increasing atomic number and decreasing size of the lanthanoid(III) ions, while the activation volumes are almost constant around a maximum at samarium/europium.[8–11] The rates of complex formation with sulfate and acetate ions also show a maximum at about samarium.[12,13] Liquid–liquid extraction experiments indicated that instead of dividing the trivalent lanthanoid(III) ions into two octads of elements with gadolinium common to both, four tetrads intersecting at neodymium/prometium, gadolinium, and holmium/erbium could better correlate with several physicochemical properties.[14] This tetrad effect is also discerned, for example, in the stability constants of the EDTA complexes in aqueous solution (see Figure S1 in the Supporting Information).[15] An analogous tetrad effect has also been proposed for the trivalent actinoid(III) ions.[16]

No direct structural evidence has emerged for an abrupt change in hydration number in solution at the gadolinium break. Ishiguro and co-workers performed EXAFS studies on the hydrated lanthanoid(III) ions in aqueous solution, but without comparison with structures in the solid state.[17] Furthermore, the results seem biased, as the large difference reported in the mean Ln–O bond length between samarium(III) and europium(III) is not consistent with other observations. Solera et al. proposed that all lanthanoid(III) ions are twelve-coordinate in a cuboctahedral fashion in aqueous solution,[18] but no other study supports such a high coordination number.

The comparable series of hydrated lanthanoid(III) ions in crystal structures are not very informative concerning the proposed change in hydration number in aqueous solution. Two almost complete series of isomorphous crystal structures have been reported, the nonaaqualanthanoid(III) trifluoromethanesulfonates $[Ln(H_2O)_9](CF_3SO_3)_3$,[19–23] and the nonaaqualanthanoid(III) ethylsulfates $[Ln(H_2O)_9](C_2H_5OSO_3)_3$ (Ln = La–Nd, Sm–Lu).[24–26] Other series of crystal structures with nonahydrated lanthanoid(III) ions are the bromates,[27–30] and the iodides for La–Ho (except Pm).[31–34] The hydrated holmium(III) and lutetium(III) bromides and the erbium(III) and lutetium(III) iodides coordinate eight water molecules in a square-antiprismatic fashion.[34,35] In other hydrated lanthanoid(III) halides, the chloride or bromide ions are bound to the lanthanoid(III) ion. The Ln–O bond lengths in the hydrated lanthanoid(III) ions in these salts are provided in Table 1.

The rhombohedral space group for the nonahydrated lanthanoid(III) trifluoromethanesulfonate and ethylsulfate salts requires a tricapped trigonal-prismatic configuration with six equidistant bonds to the water oxygen atoms in the prism and three to the capping positions (Table 1). The Ln–O(prism) bond length is only slightly shorter (by 0.1 Å) than Ln–O(cap) for the large ions at the beginning of the series, but the difference increases with increasing atomic number. Also, the mean Ln–O bond length decreases in reflection of the decreasing ionic radius in the lanthanoid series (Figure 1). A recent detailed crystallographic and 2D solid-state NMR investigation of the hydrated trifluoromethanesulfonate salts showed reduced occupancy of the capping positions for the heavy lanthanoid(III) ions Er–Lu.[23] This water deficiency starts at holmium(III) with 2.91 water molecules in the three capping positions, reported in this study, and increases for erbium(III), thulium(III), ytterbium(III), and lutetium(III) with 2.96, 2.8, 2.7, and 2.4 water molecules, respectively.[23] The hydrated lanthanoid(III) ions in the bromate salts also crystallize as tricapped trigonal prisms, but with much smaller differences between the Ln–O bond lengths in the prismatic and capping positions (Table 1). The light and large hydrated lanthanoid(III) ions in the iodide

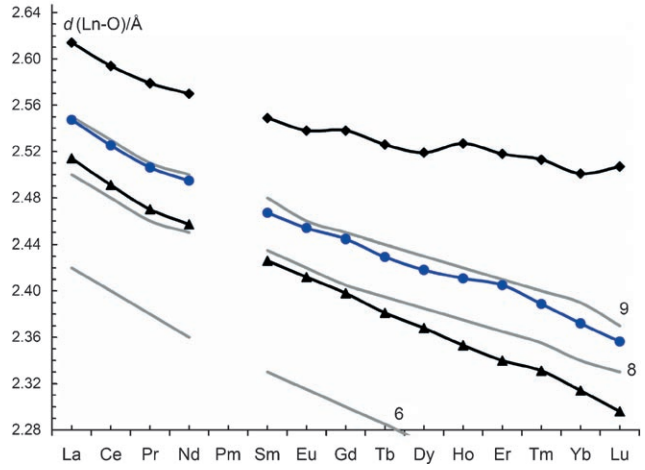

Figure 1. Crystallographic mean Ln–O bond lengths in $[Ln(H_2O)_9](CF_3SO_3)_3$ and $[Ln(H_2O)_9](C_2H_5OSO_3)_3$; the averages for the prismatic and capping positions are marked with black triangles and black diamonds, respectively, and the weighted average of all Ln–O bond lengths with filled blue circles. The gray lines represent expected mean Ln–O bond lengths calculated from the oxygen radius of coordinated water[46] and the ionic radii for six-, eight-, and ninefold coordination[45].

salts (Ln = La–Ho) are nine-coordinate in tricapped trigonal-prismatic configurations with a narrow distribution of the Ln–O bond lengths ($\leq$0.04 Å). The eight-coordinate hydrated lanthanoid(III) ions in the bromide and iodide salts with square-antiprismatic configuration display fairly wide bond-length distributions of about 0.10 and 0.05 Å, respectively (Table 1),[34,35] as is also found for the hydrated yttrium(III) ion in its solid hydrates.[36]

A combined crystallographic and 2D solid-state NMR study on octaaquascandium(III) trifluoromethanesulfonate $[Sc(H_2O)_{8.0}](CF_3SO_3)_3$ also showed a tricapped trigonal-prismatic configuration around the small lanthanoid-like scandium(III) ion at room temperature. Six water molecules form the trigonal prism (Sc–O(prism) 2.17 Å), and the remaining two water molecules appeared to be randomly distributed over the three equivalent capping crystallographic sites with an Sc–O(cap) distance of 2.43 Å.[23,37] The structural parameters obtained from an EXAFS study showed a somewhat different configuration with one capping water molecule close to the scandium(III) ion at an Sc–O(cap) bond length of 2.32 Å, and the other more distant, at about 2.55 Å.[37] The low-temperature crystal structure of $[Sc(H_2O)_{8.0}](CF_3SO_3)_3$, after a reversible phase transition to a lower symmetry space group with nine times larger unit cell, shows coordination which resembles that obtained by EXAFS at room temperature and in aqueous solution. In the low-temperature crystal structure the average Sc–O bond length to the water molecules in the prism is 2.19 Å, and the Sc–O bond lengths to the sites of the capping water molecules are 2.29, 2.54, and 2.58 Å, of which the last two have occupancy factors close to 0.5.[37] Thus, the room-temperature crystal structure is yet another example that an average of randomly distributed configurations may result in too high crystallographic symmetry for a proper description of the molecular structure; other examples are described elsewhere.[38] This phenomenon has been further elucidated in this work by using EXAFS as a lattice-independent structural probe.

The aim of the present study was to determine the coordination and structure of the hydrated lanthanoid(III) ions in aqueous solution, and thereby investigate whether there is a structural background to the proposed gadolinium break, and also to the tetrad effect. For this purpose, EXAFS data were collected at the Ln K and L_3 X-ray absorption edges of the $[Ln(H_2O)_n](CF_3SO_3)_3$ compounds, where $n = 9.0$ for Ln = La–Nd and Sm–Dy, 8.91 for Ho, 8.96 for Er, 8.8 for Tm, 8.7 for Yb, and 8.2 for Lu, and of aqueous solutions of these salts. The crystal structures of $[Lu(H_2O)_{8.2}](CF_3SO_3)_3$ at ambient temperature and 100 K were examined to provide coordination models, and the crystal structure of $[Ho(H_2O)_{8.91}](CF_3SO_3)_3$ at ambient temperature was re-determined because of the deviation of the previously reported Ho–O bond lengths from the expected trend.

Results and Discussion

Crystal structure of nonaaquaholmium(III) trifluoromethanesulfonate (S10): The structure was solved in the space group $P6_3/m$ with direct methods using SHELXS97 and SHELXL97.[39] Full-matrix least-squares refinements with anisotropic displacement parameters for all non-hydrogen atoms allowed the hydrogen atoms to be located in the list of residual peaks. The final residuals were $R_1 = 0.021$ and $wR_2 = 0.057$. The $[Ho(H_2O)_9]^{3+}$ entity is shown in Figure 2a,

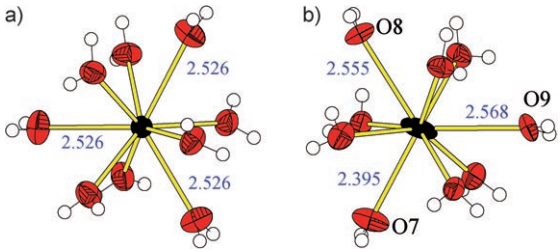

Figure 2. a) Structures of the hydrated holmium(III) ion and b) the hydrated lutetium(III) ion in the trifluoromethanesulfonate salts with 50% probability ellipsoids (hydrogen atoms with arbitrary radius). Note that only the bond lengths to the capping positions are given.

drawn by DIAMOND.[40] The Ho–O bond lengths are 2.353(2) Å for the trigonal prism and 2.526(2) Å to the sites of the capping oxygen atoms, which show nearly full occupancy, refined to 0.97(1).

Crystal structure of $[Lu(H_2O)_{8.2}](CF_3SO_3)_3$ (S13) at 100 K: The transition to the space group $R\bar{3}$ at low temperature (see Experimental Section) resulted in $Z = 18$ (versus $Z = 2$ in $P6_3/m$ at room temperature),[23] with approximately $\sqrt{3}\cdot\sqrt{3}\cdot 3$ times longer unit cell axes. The crystal structure was solved and refined in the same way as above to the final

residuals $R_1 = 0.055$ and $wR_2 = 0.154$. The structure comprises $[Lu(H_2O)_{8.2}]^{3+}$ complexes (Figure 2b) and trifluoromethanesulfonate ions, whereby the coordinated water molecules in the nine sites around the lutetium ion form strong hydrogen bonds to the sulfonate oxygen atoms, as described in detail previously.[23] The six Lu–O bond lengths in the fairly regular trigonal prism are in the range 2.272(4)–2.296(4) Å (av 2.282 Å). One capping site (O7) is fully occupied with Lu–O 2.395(4) Å, while for the two more distant capping sites (Lu–O8 2.555(6), Lu–O9 2.568(6) Å), the occupancy factors are 0.58(1) and 0.59(1), respectively. Significant residual electron density remains at about 0.7 Å from the lutetium atom between the capping sites O7/O8 and O7/O9 (see Figure 3, calculated and drawn by PLATON[41]). Furthermore, the anisotropic ellipsoidal representation of the lutetium ion is strongly elongated in the plane of the capping water molecules perpendicular to the short Lu–O7 bond.

The above observations are consistent with displacement of the lutetium ion from the center of the prism in the cases where one of the capping water molecules is absent, that is, in about 80% of the $[Lu(H_2O)_{8.2}]^{3+}$ complexes. This means that the true Lu–O bond lengths to capping water molecules in the individual complexes having two capping water molecules, that is, about 80% of the complexes, are somewhat shorter than the distances obtained by crystallography, and in agreement with the distances obtained by EXAFS (see below). The Lu–O bond lengths of the individual complexes with three capping water molecules, that is, about 20% of the complexes, are very close to values obtained in the low-temperature crystal structure.

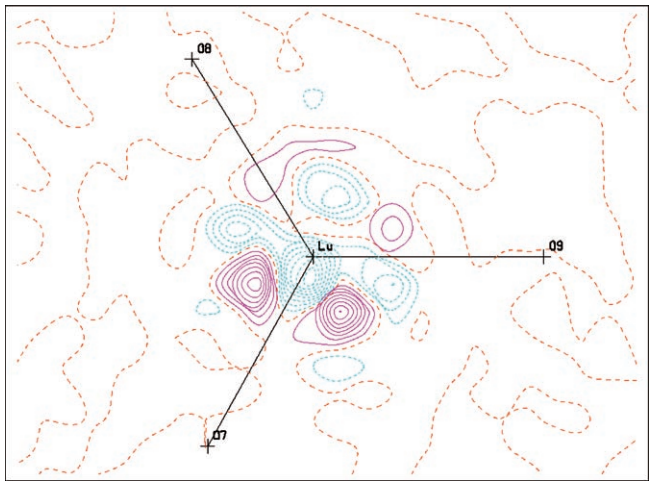

Figure 3. Residual electron density mapped in the plane of the three capping oxygen atoms.

EXAFS at lanthanoid K and L_3 edges: Structural parameters obtained from the K- and L_3-edge data are in very close agreement (see Table 3). However, the L_2 edge restricts the k range of the L_3 data,[42] to only about 9 $Å^{-1}$ for lanthanum and about 15 $Å^{-1}$ for lutetium. Furthermore, especially for the lighter lanthanoids, unusually strong double-electron excitations, $2p4d \rightarrow 5d^2$,[18,43] which are known to introduce errors in structural parameters, appear in the L_3-edge k range. The high energies of the K edges for the lanthanoids of 39 (La) to 62 keV (Lu) result in a wide core-hole state, which significantly damps the EXAFS oscillations at high k. However, after correction the longer k range in the K-edge data enables better resolution of the Ln–O bond lengths.[44] The properties and treatment of high-energy data, including a more detailed comparison of K- and L_3-edge data for the lanthanoids, are discussed in the following paper.[44]

The EXAFS data analysis at the L_3 and K edges for the hydrated neodymium(III) and lutetium(III) ions in $[Nd(H_2O)_9](CF_3SO_3)_3$ and $[Lu(H_2O)_{8.2}](CF_3SO_3)_3$ is exemplified in Figure 4. Least-squares model fitting to the EXAFS spectra was performed in the range $k = 2.4$–16.3 $Å^{-1}$ for the K edges, and in more restricted k intervals for the L_3 edges

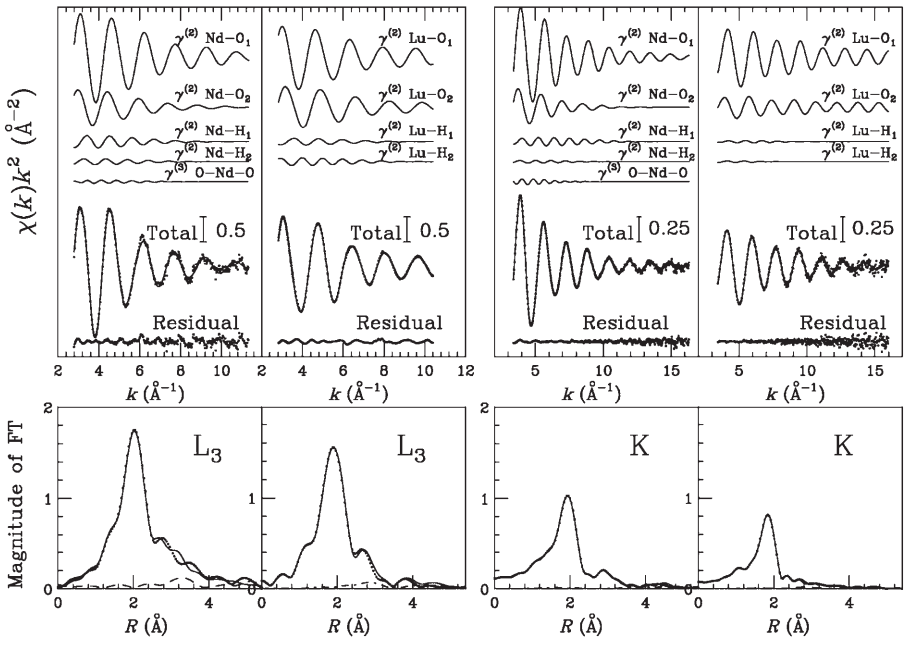

Figure 4. Fit of the K- and L_3-edge EXAFS spectra of the hydrated neodymium(III) and lutetium(III) ions in solid $[Nd(H_2O)_9](CF_3SO_3)_3$ and $[Lu(H_2O)_{8.2}](CF_3SO_3)_3$. From top to bottom in each panel, the following curves are reported: the Ln–O first-shell signals, the Ln–H first-shell signals, the O1-Ln-O1 three-body signal (only for Nd), the total model oscillation compared with the experimental spectrum, and the residual. The lower panels show the Fourier transforms without phase-shift corrections for the experimental data (dotted line), the total theoretical signals (full line), and the residual curves (dash-dotted line).

(2.8–11.3 and 2.8–10.4 $Å^{-1}$ for Nd and Lu, respectively). Various sets of structural and nonstructural parameters of the models were refined to find satisfactory agreement between the calculated and the experimental signals. Analyses of the K- and L_3-edge EXAFS spectra with a two-shell model of oxygen coordination are shown in the upper panels of Figure 4. The first four curves from the top of each panel represent the Ln–O and Ln···H first-shell contributions, and in the case of Nd the multiple scattering oscillations associated with the three short-bond O–Nd–O configurations are also included. The total model contributions match the experimental EXAFS oscillations very well, both for the K- and L_3-edge spectra, as shown in Figure 4. The Ln–O first-shell signals dominate, even though the hydrogen atoms of the first hydration shell give rise to detectable signals consistent with a well-ordered structure of the coordinated water molecules. The corresponding k^2-weighted Fourier transforms (FT) without phase shift correction are shown in the lower panels of Figure 4. The amplitudes of the L_3-edge FTs are almost twice as large as those of the K edges, due to the damping at the K edges associated with the short core-hole lifetime.

Hydrated lanthanoid(III) ions in the trifluoromethanesulfonate salts: The refined structural parameters for the EXAFS models of the hydrated lanthanoid(III) ions agree within estimated error limits with those for the the corresponding $[Ln(H_2O)_9](CF_3SO_3)_3$ crystal structures for the largest ions, Ln = La–Nd (Tables 1 and 3, cf. Figure 5). The Fourier transforms (Figure 6) show decreasing mean Ln–O bond lengths with increasing atomic number. The mean Ln–O distance from the single-shell models and the weighted mean from the two-shell models agree closely with the expected Ln–O bond lengths derived from the ionic radii of these ions in ninefold coordination and the radius of the water oxygen atom bound to trivalent metal ions (Figure 5).[45,46]

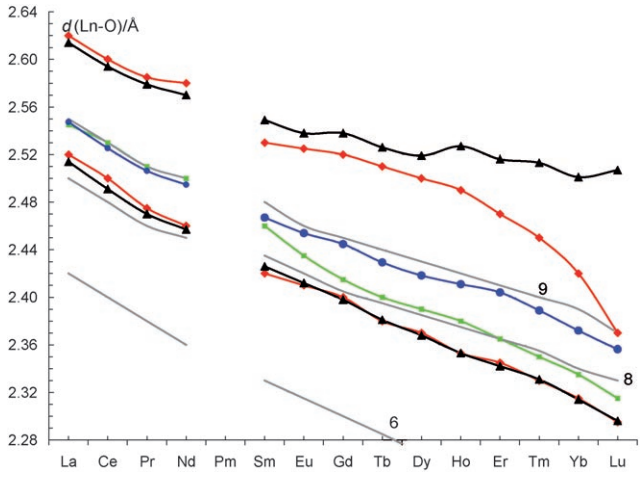

Figure 5. EXAFS results for the hydrated lanthanoid(III) ions in the solid trifluoromethanesulfonate salts (Table 3). The mean $Ln–O_{prism}$ and $Ln–O_{capping}$ bond lengths from two-shell fits are marked with red rhombuses (top line and bottom line, respectively), and the mean Ln–O bond lengths from one-shell fits with green squares. Other labels are as in Figure 1.

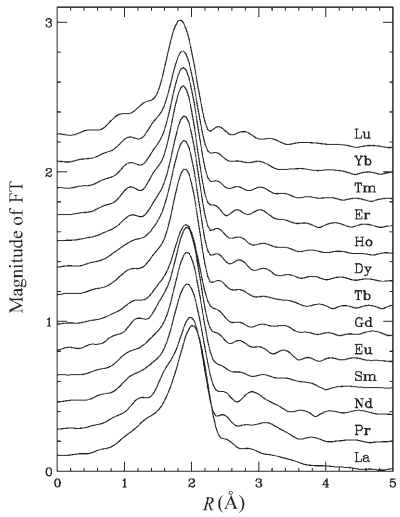

Figure 6. Fourier transforms (without phase-shift correction) of the hydrated lanthanoid(III) ions in the solid trifluoromethanesulfonate salts.

With decreasing size of the central metal ion, repulsion between the prism and capping water molecules increases.[23] As a result, the occupancy of the capping sites starts to decrease with increasing atomic number for $[Ln(H_2O)_n](CF_3SO_3)_3$ (Ln = Ho–Lu). For the solid compounds with water deficit $[Ln(H_2O)_n](CF_3SO_3)_3$ [Ln = Ho, $n = 8.91(3)$ from the refined occupancy factors (see above), Er 8.96(5), Tm 8.8(1), Yb 8.7(1),[23] and Lu 8.2(1)], the Ln–O bond lengths in the prism from the crystal structures in $P6_3/m$ agree closely with those obtained from EXAFS (Tables 1 and 3, Figure 5).

For the smallest ion, lutetium(III), the EXAFS functions of $[Lu(H_2O)_{8.2}](CF_3SO_3)_3$ (**S14**) at room temperature and of the aqueous solution **L14** are quite similar (Figure 7). Furthermore, the refined EXAFS models for **S14** at room temperature and **L14** are consistent with the distorted configuration of the hydrated ion in the low-temperature (100 K) crystal structure of **S14**. A similar distorted structure with low occupancy of two more distant capping sites was also found for the low-temperature phase of $[Sc(H_2O)_{8.0}](CF_3SO_3)_3$.[37] Thus, the high symmetry ($P6_3/m$) of the crystal structure of **S14** at room temperature is an average corresponding to a random distribution of the capping water molecules with a concomitant displacement of the central lanthanoid ion. Such a model would explain the sharp decrease in the mean Ln–O bond length for the capping water molecules in the last tetrad (Ln = Ho–Lu, Figure 5). The most weakly bound capping water molecules have too-large Debye–Waller factors, due to weak bonding with a large bond-length distribution, observable by EXAFS. The slightly shorter mean Lu–O bond length of 2.370(8) Å to the most strongly bound capping water molecule observed by EXAFS in comparison to that obtained crystallographically (2.395(4) Å) is due to the fact that the lutetium atom has a

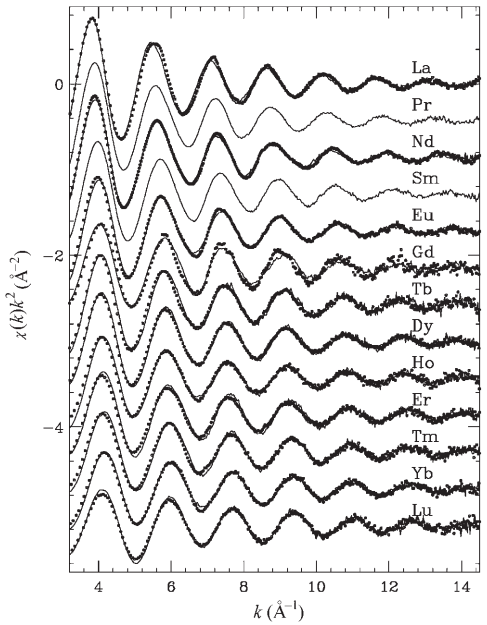

Figure 7. Comparison of the raw EXAFS spectra of the hydrated lanthanoid(III) ions in the solid trifluoromethanesulfonate salts and in aqueous solution. The solid lines represent the aqueous solutions, and the dots the solid compounds.

mean position of two alternatives in the crystallographic description for about 80% of the complexes with only two capping water molecules (see above and Figure 3). This means that the true Lu–O bond length to that capping water molecule is shorter than that determined crystallographically, and that the bond length obtained by EXAFS for **S14** at room temperature and in aqueous solution of 2.37(1) and 2.35(1) Å (Table 3), respectively, seems more correct.

For the medium-sized lanthanoid ions (Sm–Ho), the refined EXAFS Ln–O bond lengths within the prism are again in satisfactory agreement with those obtained from the corresponding $[Ln(H_2O)_9](CF_3SO_3)_3$ crystal structures (Tables 1 and 3). However, the mean capping bond length from the EXAFS data is somewhat shorter, especially for Dy and Ho, than the crystallographic result (Figure 5). This deviation indicates a somewhat distorted molecular configuration, probably with one capping water molecule that is more strongly bound and thus contributes more to the EXAFS function. Furthermore, the mean Ln–O bond lengths from the EXAFS single-shell fit are shorter than expected from the sum of the ionic radii of the lanthanoid(III) ion in ninefold coordination and the water oxygen atom,[45,46] and for holmium it even approaches the expected value for eightfold coordination (see Figure 5).

Even though the hydrated lanthanoid(III) ions of the $[Ln(H_2O)_9](CF_3SO_3)_3$ compounds in the third tetrad (Ln = Gd–Ho) show no or very small water deficits, their structures are affected by the decreasing ionic radius of the metal ion. Their intermediate size evidently allows unequal bond strength to the three capping water molecules by some displacement of the lanthanoid ion from the center of the prism, as for the smaller water-deficient lanthanoid ions starting at holmium. This displacement would cause increasing asymmetry of the three capping sites and probably also reduced symmetry of the trigonal prism. An averaged random distribution will again cause the symmetry of the crystal structures to appear higher than the true symmetry of the molecular complexes. The EXAFS method, in which the interference pattern of the scattering depends on the instantaneous interatomic distances, is lattice-independent and can provide more realistic values for well-defined Ln–O bond lengths within the molecular complexes. However, loosely bound atoms in the capping positions with large Debye–Waller coefficients would contribute less to the EXAFS signal, and the shorter bonds more to the observed Ln–O(capping) bond lengths, so that the apparent distance is shorter than the true mean value. Unfortunately, the difference in bond length of these capping water molecules is too small to be resolved by the EXAFS technique.

The proposed bonding schemes of the capping water molecules in the hydrated lanthanoid(III) ions in the four tetrads is depicted schematically in Figure 8. The increasing asymmetry may also affect the previously discussed hydrogen bonding to the surroundings,[37] both in the solid state and in aqueous solution.

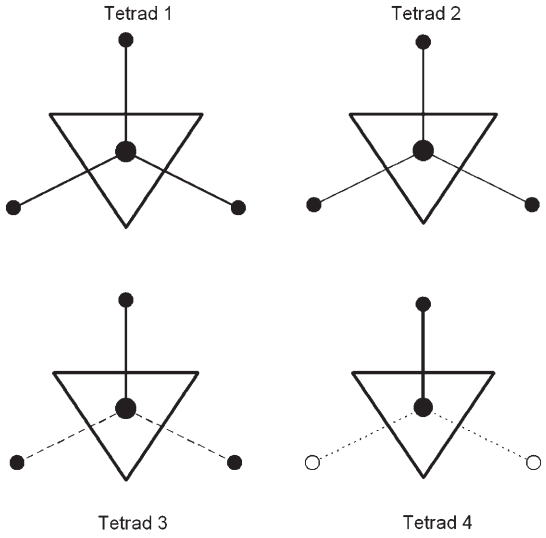

Figure 8. Schematic illustration for the four tetrads of typical changes in the capping positions of the hydrated lanthanoid(III) ions. The line thickness represents the bond strength, and an open circle a less than fully occupied site.

The hydrated lanthanoid(III) ions in aqueous solution: The EXAFS spectra for each hydrated lanthanoid(III) ion in aqueous solution and in the solid $[Ln(H_2O)_n](CF_3SO_3)_3$ compound overlap closely (Figure 7). The refined structural parameters are also similar (Table 3), including those of the heavy lanthanoid(III) ions in the water-deficient $[Ln(H_2O)_n](CF_3SO_3)_3$ solid compounds (Ln = Ho–Lu, see Figure 5). The similarities strongly indicate that the hydrated lanthanoid(III) ions in aqueous solution also maintain a similar tricapped trigonal-prismatic configuration with water de-

ficiency in the capping positions for the smallest ions. Consequently, the structural models derived from the solid $[Ln(H_2O)_n](CF_3SO_3)_3$ compounds are excellent models for the description of the structures of the hydrated lanthanoid(III) ions in aqueous solution. These results also show the presence of an equilibrium between eight- and nine-coordinate hydrated lanthanoid(III) ions, with di- and tricapped trigonal-prismatic configuration, respectively, for the lanthanoids heavier than dysprosium in aqueous solution. The fraction of eight-coordinated hydrated ions increases with increasing atomic number of the lanthanoids. The hydrated lanthanoid(III) ions lighter than holmium are nine-coordinate in more or less regular tricapped trigonal-prismatic configurations in aqueous solution, and the regularity of the tricapped trigonal prisms increases with decreasing atomic number.

The gadolinium break and tetrad hypotheses: The combined EXAFS and crystallographic results show that all hydrated lanthanoid(III) ions, both in solid $[Ln(H_2O)_9](CF_3SO_3)_3$ salts and in aqueous solution, are surrounded by water molecules in capped trigonal-prismatic configurations. For the largest ions (La–Nd), the mean bond lengths from the EXAFS studies on the solid $[Ln(H_2O)_9](CF_3SO_3)_3$ compounds agree with the crystallographic distances. Furthermore, the EXAFS distances from the corresponding aqueous solutions, where the Ln–O(cap) bond length is about 0.10 Å longer than Ln–O(prism), are in very good agreement, consistent with a regular tricapped trigonal prism.

At samarium the difference between the Ln–O(prism) and Ln–O(cap) bond lengths starts to increase with increasing atomic number (Figure 5). From the crystal structures of the solid $[Ln(H_2O)_9](CF_3SO_3)_3$ and $[Ln(H_2O)_9](C_2H_5OSO_3)_3$ compounds solved in the high-symmetry space group $P6_3/m$, the Ln–O(cap) bond lengths appear almost constant, while the Ln–O(prism) bond lengths gradually decrease. On the other hand, the lattice-independent EXAFS measurements show that the mean Ln–O(cap) bond lengths actually decrease gradually in a similar way to the Ln–O(prism) bond lengths as long as the capping positions are fully occupied, that is, up to Dy (Figure 5). This divergence between the two groups of bond lengths increases rapidly with increasing atomic number in the last tetrad (Ln = Ho/Er–Lu), with water deficiency.

The different values for the Ln–O(prism) bond lengths obtained in EXAFS and crystallographic studies for the smallest lanthanoid(III) ions are consistent with one of the three capping water molecules approaching the central metal ion by expanding one of the rectangular sides of the trigonal prism.[23] The distortion increases the disorder parameter σ^2 of the Ln–O(prism) bond lengths for Tm–Lu to values even larger than those for the strongly bound capping oxygen atom (Table 3).

These structural studies on hydrated lanthanoid(III) ions in solid $[Ln(H_2O)_9](CF_3SO_3)_3$ compounds and in aqueous solution indicate at least two principal structural changes in the series of hydrated lanthanoid(III) ions with increasing atomic number. The first, starting at samarium, is evidenced by the more rapid decrease in the mean Ln–O bond length obtained by EXAFS versus that from the crystal structures, and is most probably caused by unequal bond strength to the capping positions. Another structural change starts at holmium, where one of the capping water sites may become partially unoccupied. Whether such structural effects could cause the irregularities in the physicochemical properties observed by Spedding and co-workers is not clear. However, the hydrogen-bonding arrangement around the hydrated lanthanoid(III) ions may change significantly, and the more weakly bound capping water molecules would become more labile. In any case, the present study shows very clearly that there is no sudden change in the coordination number of the hydrated lanthanoid(III) ions anywhere in the series. The most significant change in the structure of the hydrated lanthanoid(III) ions along the series occurs at holmium, the first hydrated lanthanoid(III) ion with a mean coordination number less than nine in its tricapped trigonal-prismatic configuration. That structural effect is also present in aqueous solution, and the true hydration number of the heaviest lanthanoid(III) ions is certainly lower than nine, even though basically a capped trigonal prism is retained. The changes starting at samarium and possibly at gadolinium, as discussed above, could fit to the tetrad model. Thus, the structural effects at the tetrad nodes neodymium/promethium and gadolinium are most probably due to changes in symmetry and/or hydrogen bonding of the nonahydrated lanthanoid(III) ions, while the holmium/erbium node corresponds to a gradual decrease in coordination number.

Conclusion

The EXAFS structures of the hydrated lanthanoid(III) ions in aqueous solution resemble those of the solid nonaaqualanthanoid(III) trifluoromethanesulfonate compounds, $[Ln(H_2O)_n](CF_3SO_3)_3$ ($n = 9.0$ for Ln = La–Nd and Sm–Dy, 8.91 for Ho, 8.96 for Er, 8.8 for Tm, 8.7 for Yb, and 8.4 (8.2 at 100 K) for Lu). The basic configuration of the water oxygen atoms is a tricapped trigonal prism, in which especially the bonding to the capping water molecules varies along the lanthanoid series. The capping water molecules are equidistant for the largest lanthanoid(III) ions (La–Nd). Starting at samarium, distortions from regular symmetry become noticeable and increase up to dysprosium. For the smallest lanthanoid(III) ions with water deficiency (Ho–Lu), one of the capping water molecules becomes more strongly bound, and the occupancy of the other two sites starts to decrease. The structure of the hydrated lutetium(III) ion can basically be described as seven-coordinate with a strong bond to a capping water molecule at 2.37 Å, only 0.08 Å longer than the group of six Lu–O(prism) distances to a prism that is distorted to allow the short Ln–O(cap) bond. The partial occupancy of the two more distant capping sites correspond to displacement of the lutetium(III) ion, and the remaining capping water molecules are hardly observable by EXAFS. This distorted structure of the hydrated

lutetium(III) ion resembles the 7+1 coordination of the hydrated scandium(III) ion with Sc–O bond lengths of 2.32 and about 2.55 Å to two capping water molecules, previously observed by EXAFS.[37] The catalytic properties of the scandium(III) ion and the heavy lanthanoid(III) ions in, for example, carbon–carbon bond formation reactions in aqueous media[47] are probably connected to the asymmetry and the water deficiency in the capping positions.

There is no sudden change in hydration number along the series of the hydrated lanthanoid(III) ions in aqueous solution. The most marked structural change starts at holmium(III) with gradually increasing water deficiency in the capping positions, and not at the proposed gadolinium break. The structural effects can be divided into tetrads with equivalent capping water molecules in the first tetrad, and with one capping water molecule strongly bound in the fourth tetrad. In the second and third tetrads the symmetry of the tricapped trigonal prisms gradually decreases, possibly with a change in the hydrogen bonding at gadolinium.

Experimental Section

Chemicals: Anhydrous lanthanoid(III) trifluoromethanesulfonates Ln$(CF_3SO_3)_3$ (Ln = La–Nd, Sm, Gd–Lu) were purchased (Aldrich) or prepared by dissolving the corresponding lanthanoid(III) oxide Ln_2O_3 (Aldrich) in aqueous trifluoromethanesulfonic acid (Fluka). After dissolving the oxides, the solutions were filtered and the excess of water and acid boiled off in an oven at 470 K, and the anhydrous salts were stored at 470 K. Deionized and MilliPore-filtered water was used.

Sample preparation: Crystals of nonaaqualanthanoid(III) trifluoromethanesulfonates (Ln = La–Nd, Sm–Lu) were prepared by dissolving the corresponding anhydrous salt in dilute trifluoromethanesulfonic acid (pH $\approx$1), followed by slow evaporation. Analyses of the hydrated trifluoromethanesulfonate salts for Ln = Er–Lu showed that the water content at ambient temperature was less than nine: Er 8.96(5), Tm 8.8(1), Yb 8.7(1), and Lu 8.4(1).[23] In this work we obtained 8.2(1) water molecules at 100 K in the crystal structure of $[Lu(H_2O)_{8.2}](CF_3SO_3)_3$ by refining the occupancy factors. To avoid hydrolysis the corresponding aqueous solutions were prepared by dissolving weighed amounts of the hydrated trifluoromethanesulfonate salts in a known volume of 0.1 mol dm^{-3} aqueous trifluoromethanesulfonic acid; the acidity constants (pK_a) of the hydrated lanthanoid(III) ions in aqueous solution are reported to be in the range from 8.5 (La) to 7.6 (Lu).[48] The densities of the solutions were measured with an Anton Paar DMA 35 densitometer. Labels and chemical composition of the crystalline hydrates and the aqueous solutions studied by EXAFS are provided in Table 2.

Crystallographic data collection: A single crystal of $[Ho(H_2O)_{8.91}](CF_3SO_3)_3$ was enclosed within a thin-walled capillary and measured at ambient temperature. For $[Lu(H_2O)_{8.2}](CF_3SO_3)_3$ several single-crystal measurements were performed, the first with a rather rapid cooling cycle, approximately 30 min from 300 to 100 K. However, the phase transition expected from the DSC measurements[23] did not occur. In the second experiment a set of short data collections (15 min) was performed, from 263 down to 113 K with 10 K interval and 15 min dwell time at each temperature. The unit cell was determined at each 10 K step and the phase transition was observed at approximately 130 K. Final data collection was performed at 100 K. All data collections were performed with an Oxford Diffraction Excalibur-II κ diffractometer equipped with a Sapphire-III CCD detector[49] using ω-scans at different φ settings.

EXAFS data collection: EXAFS measurements on the aqueous solutions **L1**–**L14**, and the crystalline hydrates $[Ln(H_2O)_n](CF_3SO_3)_3$ (**S1**–**S14**) were performed at both the Ln K and L_3 X-ray absorption edges. The K-edge data were collected at the bending magnet beam line BM29 at the European Synchrotron Radiation Facility (ESRF), Grenoble, France,[42] which was operated at 6.0 GeV in 16-bunch mode and a maximum current of 80 mA. The Ln L_3-edge measurements were performed at the wiggler beam line 4-1 at the Stanford Synchrotron Radiation Laboratory (SSRL), Stanford, USA, which was operated at 3.0 GeV and a maximum current of 100 mA. The EXAFS stations at ESRF and SSRL were equipped with Si[511] and Si[111] double-crystal monochromators, respectively. Higher order harmonics were reduced by detuning the second monochromator crystal to reflect at the end of the scans, 80% of maximum intensity at the K-edge energies, and 30–50% of maximum intensity at the L_3 edges, with the lower value at lower energy. Internal energy calibration was made when possible with a foil of the corresponding lanthanoid metal.[50] Transmission mode was used for the K-edge measurements, while for the L_3 edges simultaneous data collection was performed both in transmission and fluorescence mode. A Lytle fluorescence detector without X-ray filter was used for the lightest lanthanoid elements, including an appropriate transition metal oxide fluorescence filter for Sm–Lu, using a very gentle flow of argon and/or krypton gas depending on energy. For each sample 3–4 scans were averaged after energy calibration by means of the EXAFSPAK program package.[51]

Table 2. Labels, chemical composition, and Ln–O bond lengths from crystallographic studies[19–23] used in the EXAFS studies.

Label	Sample	r(Ln–O) [Å]
S1	$[La(OH_2)_9](CF_3SO_3)_3$	2.548 (6×2.515, 3×2.614)
S2	$[Ce(OH_2)_9](CF_3SO_3)_3$	2.525 (6×2.499, 3×2.594)
S3	$[Pr(OH_2)_9](CF_3SO_3)_3$	2.506 (6×2.470, 3×2.579)
S4	$[Nd(OH_2)_9](CF_3SO_3)_3$	2.490 (6×2.451, 3×2.568)
S5	$[Sm(OH_2)_9](CF_3SO_3)_3$	2.464 (6×2.422, 3×2.549)
S6	$[Eu(OH_2)_9](CF_3SO_3)_3$	2.452 (6×2.408, 3×2.536)
S7	$[Gd(OH_2)_9](CF_3SO_3)_3$	2.444 (6×2.397, 3×2.538)
S8	$[Tb(OH_2)_9](CF_3SO_3)_3$	2.429 (6×2.380, 3×2.527)
S9	$[Dy(OH_2)_9](CF_3SO_3)_3$	2.416 (6×2.364, 3×2.520)
S10	$[Ho(OH_2)_{8.91}](CF_3SO_3)_3$	2.421 (6×2.368, 3×2.527)
S11	$[Er(OH_2)_{8.95}](CF_3SO_3)_3$	2.399 (6×2.340, 2.95×2.518)
S12	$[Tm(OH_2)_{8.8}](CF_3SO_3)_3$	2.386 (6×2.322, 2.8×2.522)
S13	$[Yb(OH_2)_{8.7}](CF_3SO_3)_3$	2.376 (6×2.303, 2.7×2.538)
S14	$[Lu(OH_2)_{8.4}](CF_3SO_3)_3$	2.359 (6×2.288, 2.2×2.510)
L1	0.2 mol dm^{-3} $[La(OH_2)_9](CF_3SO_3)_3$ in 0.1 mol dm^{-3} CF_3SO_3H	
L2	0.2 mol dm^{-3} $[Ce(OH_2)_9](CF_3SO_3)_3$ in 0.1 mol dm^{-3} CF_3SO_3H	
L3	0.2 mol dm^{-3} $[Pr(OH_2)_9](CF_3SO_3)_3$ in 0.1 mol dm^{-3} CF_3SO_3H	
L4	0.2 mol dm^{-3} $[Nd(OH_2)_9](CF_3SO_3)_3$ in 0.1 mol dm^{-3} CF_3SO_3H	
L5	0.2 mol dm^{-3} $[Sm(OH_2)_9](CF_3SO_3)_3$ in 0.1 mol dm^{-3} CF_3SO_3H	
L6	0.2 mol dm^{-3} $[Eu(OH_2)_9](CF_3SO_3)_3$ in 0.1 mol dm^{-3} CF_3SO_3H	
L7	0.2 mol dm^{-3} $[Gd(OH_2)_9](CF_3SO_3)_3$ in 0.1 mol dm^{-3} CF_3SO_3H	
L8	0.2 mol dm^{-3} $[Tb(OH_2)_9](CF_3SO_3)_3$ in 0.1 mol dm^{-3} CF_3SO_3H	
L9	0.2 mol dm^{-3} $[Dy(OH_2)_9](CF_3SO_3)_3$ in 0.1 mol dm^{-3} CF_3SO_3H	
L10	0.2 mol dm^{-3} $[Ho(OH_2)_9](CF_3SO_3)_3$ in 0.1 mol dm^{-3} CF_3SO_3H	
L11	0.2 mol dm^{-3} $[Er(OH_2)_{8.95}](CF_3SO_3)_3$ in 0.1 mol dm^{-3} CF_3SO_3H	
L12	0.2 mol dm^{-3} $[Tm(OH_2)_{8.8}](CF_3SO_3)_3$ in 0.1 mol dm^{-3} CF_3SO_3H	
L13	0.2 mol dm^{-3} $[Yb(OH_2)_{8.7}](CF_3SO_3)_3$ in 0.1 mol dm^{-3} CF_3SO_3H	
L14	0.2 mol dm^{-3} $[Lu(OH_2)_{8.4}](CF_3SO_3)_3$ in 0.1 mol dm^{-3} CF_3SO_3H	

EXAFS data analysis: The EXAFSPAK[51] and GNXAS[52,53] program packages were used for data treatment. The GNXAS code is based on the calculation of the EXAFS signal and subsequent refinement of the structural parameters.[52,53] The GNXAS method accounts for multiple scattering (MS) paths by including the configurational average of all the MS signals to allow fitting of correlated distances and bond length variances described by Debye–Waller factors. A detailed description of the distribution of the ion–solvent distances in a coordination shell should in principle take asymmetry into account.[54,55] Therefore the Ln–O two-body signals associated with the first coordination shells were modeled with Γ-like distribution functions, which depend on four parameters, the coordination number N, the centroid distance R (the first moment of the function $4\pi \int g(r) r^2 dr$), the mean-square variation in the mean distance σ, and the skewness parameter β. Details of the GNXAS data analysis, in

particular for the high-energy K-edge data, are reported elsewhere.[44] Since the structure of the hydrated lanthanoid(III) ions can be described as a capped trigonal prism, two models were applied: a two-shell model with separate Ln–O(prism) and Ln–O(cap) distances, and a single-shell model allowing for an asymmetric distribution around a centroid Ln–O distance.

The results of the refinements of the hydrated lanthanoid(III) ion in the solid $[Ln(H_2O)_n](CF_3SO_3)_3$ compounds and in aqueous solution obtained with the program packages GNXAS and EXAFSPAK agree within the limits of error and are summarized in Table 3 and Table S1 in the Supporting Information. The results presented in the figures are from the refinements made by the GNXAS program, which allows fitting of asymmetric distance distributions, and also fitting of the splines to reduce spurious peaks in the Fourier transforms.

The standard deviations reported for the refined parameters in Table 3 were obtained from k^2-weighted least-squares refinements of the EXAFS function $\chi(k)$ and do not include systematic errors of the measurements. These statistical error values allow reasonable comparisons of, for exam-

Table 3. EXAFS structural parameters of the hydrated lanthanum(III) and lanthanoid(III) ions in the solid trifluoromethanesulfonate salts and in slightly acidic aqueous solution, as determined by GNXAS by means of two models: two shells for a capped trigonal prism with six prism water molecules and up to three capping water molecules, and a single-shell model with an average of all Ln–O bond lengths. The refinements allowed asymmetric Ln–O bond-length distributions with the peak maximum R_m [Å] given in parentheses, the third cumulant C_3 [Å^3], and the Debye–Waller factor coefficient σ^2 [Å^2]. The number of distances N was not refined.

	K-edge data			L_3-edge data		
	Two-shell fit		One-shell fit	Two-shell fit		One-shell fit
	Ln–O_{prism}	Ln–$O_{capping}$	Ln–O	Ln–O_{prism}	Ln–$O_{capping}$	Ln–O
$[La(H_2O)_9](CF_3SO_3)_3$(s); d(La–O)$_{prism}$ = 2.515 Å, d(La–O)$_{capping}$ = 2.614 Å, d(La–O)$_{mean}$ = 2.548 Å						
d	2.527 (2.520)	2.639 (2.629)	2.555 (2.543)	2.529 (2.516)	2.663 (2.621)	2.549 (2.549)
σ^2/C_3	0.0068/2.8×10^{-5}	0.0091/7.1×10^{-5}	0.0079/8.9×10^{-5}	0.0080/1.1×10^{-4}	0.093/6.4×10^{-4}	0.0074/$>1.0\times10^{-6}$
N	6	3	9	6	3	9
La^{3+}/water (acidic)						
d	2.549 (2.525)	2.641 (2.618)	2.560 (2.549)	2.531 (2.515)	2.596 (2.596)	2.560 (2.542)
σ^2/C_3	0.0070/2.7×10^{-4}	0.0091/3.0×10^{-4}	0.0086/6.1×10^{-5}	0.0063/1.5×10^{-4}	0.0075/$>1.0\times10^{-6}$	0.0107/1.1×10^{-4}
N	6	3	9	6	3	9
$[Ce(H_2O)_9](CF_3SO_3)_3$(s); d(Ce–O)$_{prism}$ = 2.491 Å, d(Ce–O)$_{capping}$ = 2.597 Å, d(Ce–O)$_{mean}$ = 2.533 Å						
d				2.509 (2.509)	2.599 (2.599)	2.547 (2.533)
σ^2/C_3				0.0076/$>1.0\times10^{-6}$	0.0081/$>1.0\times10^{-6}$	0.0106/1.4×10^{-4}
N				6	3	9
Ce^{3+}/water (acidic)						
d	2.516 (2.508)	2.601 (2.591)	2.526 (2.515)	2.491 (2.491)	2.620 (2.602)	2.540 (2.529)
σ^2/C_3	0.0067/4.0×10^{-5}	0.0089/4.2×10^{-5}	0.0090/8.7×10^{-5}	0.0055/$>1.0\times10^{-6}$	0.0145/1.1×10^{-4}	0.0071/3.8×10^{-5}
N	6	3	9	6	3	9
$[Pr(H_2O)_9](CF_3SO_3)_3$(s); d(Pr–O)$_{prism}$ = 2.470 Å, d(Pr–O)$_{capping}$ = 2.584 Å, d(Pr–O)$_{mean}$ = 2.506 Å						
d	2.480 (2.472)	2.593 (2.583)	2.520 (2.509)	2.475 (2.469)	2.613 (2.593)	2.530 (2.514)
σ^2/C_3	0.0069/2.9×10^{-5}	0.0113/3.7×10^{-5}	0.0091/4.5×10^{-5}	0.0060/1.8×10^{-5}	0.0135/2.8×10^{-4}	0.0097/3.2×10^{-4}
N	6	3	9	6	3	9
Pr^{3+}/water (acidic)						
d	2.482 (2.475)	2.639 (2.607)	2.514 (2.504)	2.475 (2.474)	2.579 (2.545)	2.507 (2.507)
σ^2/C_3	0.0068/2.9×10^{-5}	0.0101/5.2×10^{-4}	0.0091/4.5×10^{-5}	0.0070/0.3×10^{-5}	0.0112/5.2×10^{-4}	0.0097/$>1.0\times10^{-6}$
N	6	3	9	6	3	9
$[Nd(H_2O)_9](CF_3SO_3)_3$(s); d(Nd–O)$_{prism}$ = 2.457 Å, d(Nd–O)$_{capping}$ = 2.570 Å, d(Nd–O)$_{mean}$ = 2.502 Å						
d	2.471 (2.467)	2.573 (2.568)	2.519 (2.492)	2.478 (2.471)	2.581 (2.571)	2.506 (2.506)
σ^2/C_3	0.0042/1.4×10^{-5}	0.0041/1.8×10^{-5}	0.0066/2.9×10^{-4}	0.0054/2.4×10^{-5}	0.0031/4.6×10^{-5}	0.0066/$>1.0\times10^{-6}$
N	6	3	9	6	3	9
Nd^{3+}/water (acidic)						
d	2.483 (2.455)	2.574 (2.565)	2.524 (2.500)	2.466 (2.461)	2.598 (2.571)	2.527 (2.500)
σ^2/C_3	0.0065/2.9×10^{-5}	0.0080/2.9×10^{-5}	0.010/0.7×10^{-5}	0.0059/2.9×10^{-5}	0.0151/2.9×10^{-5}	0.0069/3.6×10^{-4}
N	6	3	9	6	3	9
$[Sm(H_2O)_9](CF_3SO_3)_3$(s); d(Sm–O)$_{prism}$ = 2.426 Å, d(Sm–O)$_{capping}$ = 2.550 Å, d(Sm–O)$_{mean}$ = 2.467 Å						
d				2.437 (2.426)	2.543 (2.528)	2.472 (2.461)
σ^2/C_3				0.0054/7.4×10^{-5}	0.0119/1.3×10^{-4}	0.0071/1.1×10^{-4}
N				6	3	9
Sm^{3+}/water (acidic)						
d	2.450 (2.422)	2.549 (2.526)	2.485 (2.457)	2.426 (2.419)	2.533 (2.525)	2.474 (2.464)
σ^2/C_3	0.0077/3.3×10^{-4}	0.019/7.0×10^{-5}	0.0118/4.5×10^{-4}	0.0057/2.6×10^{-5}	0.0040/3.9×10^{-5}	0.0079/3.5×10^{-4}
N	6	3	9	6	3	9
$[Eu(H_2O)_9](CF_3SO_3)_3$(s); d(Eu–O)$_{prism}$ = 2.412 Å, d(Eu–O)$_{capping}$ = 2.538 Å, d(Eu–O)$_{mean}$ = 2.457 Å						
d	2.421 (2.416)	2.524 (2.518)	2.466 (2.439)	2.423 (2.412)	2.529 (2.510)	2.436 (2.431)
σ^2/C_3	0.0057/1.0×10^{-5}	0.0064/0.6×10^{-5}	0.0074/3.2×10^{-4}	0.0100/5.6×10^{-5}	0.0172/2.2×10^{-4}	0.0041/1.3×10^{-5}
N	6	3	9	6	3	9
Eu^{3+}/water (acidic)						
d	2.422 (2.414)	2.549 (2.523)	2.448 (2.432)	2.420 (2.415)	2.565 (2.521)	2.437 (2.427)
σ^2/C_3	0.0057/6.3×10^{-5}	0.0100/3.8×10^{-4}	0.0088/1.6×10^{-4}	0.0051/4.1×10^{-5}	0.0055/1.0×10^{-4}	0.0073/5.3×10^{-5}
N	6	3	9	6	3	9

Table 3. (Continued)

	K-edge data			L_3-edge data		
	Two-shell fit		One-shell fit	Two-shell fit		One-shell fit
	$Ln-O_{prism}$	$Ln-O_{capping}$	Ln–O	$Ln-O_{prism}$	$Ln-O_{capping}$	Ln–O
$[Gd(H_2O)_9](CF_3SO_3)_3$(s); $d(Gd-O)_{prism}=2.398$ Å, $d(Gd-O)_{capping}=2.538$ Å, $d(Gd-O)_{mean}=2.445$ Å						
d	2.412 (2.405)	2.531 (2.517)	2.424 (2.415)	2.410 (2.398)	2.353 (2.521)	2.421 (2.407)
σ^2/C_3	$0.0058/2.2\times10^{-5}$	$0.0108/1.0\times10^{-4}$	$0.0085/4.1\times10^{-5}$	$0.0099/8.8\times10^{-5}$	$0.0112/1.4\times10^{-4}$	$0.0101/1.1\times10^{-4}$
N	6	3	9	6	3	9
Gd^{3+}/water (acidic)						
d	2.408 (2.400)	2.545 (2.520)	2.405 (2.395)	2.400 (2.389)	2.530 (2.521)	2.428 (2.410)
σ^2/C_3	$0.0056/3.5\times10^{-5}$	$0.0099/3.5\times10^{-4}$	$0.0071/5.0\times10^{-5}$	$0.0098/7.9\times10^{-5}$	$0.0052/5.7\times10^{-5}$	$0.0055/1.5\times10^{-4}$
N	6	3	9	6	3	9
$[Tb(H_2O)_9](CF_3SO_3)_3$(s); $d(Tb-O)_{prism}=2.381$ Å, $d(Tb-O)_{capping}=2.527$ Å, $d(Tb-O)_{mean}=2.428$ Å						
d	2.407 (2.385)	2.526 (2.491)	2.396 (2.387)	2.390 (2.382)	2.529 (2.521)	2.397 (2.390)
σ^2/C_3	$0.0056/2.1\times10^{-4}$	$0.0122/6.4\times10^{-5}$	$0.0063/2.4\times10^{-5}$	$0.0048/0.3\times10^{-5}$	$0.0134/3.2\times10^{-5}$	$0.0074/3.6\times10^{-5}$
N	6	3	9	6	3	9
Tb^{3+}/water (acidic)						
d	2.405 (2.385)	2.533 (2.491)	2.411 (2.385)	2.395 (2.387)	2.520 (2.510)	2.410 (2.396)
σ^2/C_3	$0.0069/2.1\times10^{-4}$	$0.0156/9.7\times10^{-4}$	$0.0084/3.1\times10^{-4}$	$0.0060/4.0\times10^{-5}$	$0.0078/5.4\times10^{-5}$	$0.0072/1.1\times10^{-4}$
N	6	3	9	6	3	9
$[Dy(H_2O)_9](CF_3SO_3)_3$(s); $d(Dy-O)_{prism}=2.368$ Å, $d(Dy-O)_{capping}=2.519$ Å, $d(Dy-O)_{mean}=2.418$ Å						
d	2.390 (2.377)	2.492 (2.485)	2.400 (2.391)	2.371 (2.367)	2.520 (2.510)	2.407 (2.392)
σ^2/C_3	$0.0050/8.8\times10^{-5}$	$0.0059/2.3\times10^{-5}$	$0.0074/3.2\times10^{-5}$	$0.0034/0.9\times10^{-5}$	$0.0054/6.7\times10^{-5}$	$0.0076/1.4\times10^{-4}$
N	6	3	9	6	3	9
Dy^{3+}/water (acidic)						
d	2.380 (2.372)	2.502 (2.496)	2.396 (2.385)	2.378 (2.371)	2.504 (2.494)	2.389 (2.385)
σ^2/C_3	$0.0057/2.1\times10^{-5}$	$0.0083/1.0\times10^{-5}$	$0.0074/8.8\times10^{-5}$	$0.0059/3.1\times10^{-5}$	$0.0087/5.7\times10^{-5}$	$0.0071/0.8\times10^{-5}$
N	6	3	9	6	3	9
$[Ho(H_2O)_9](CF_3SO_3)_3$(s); $d(Ho-O)_{prism}=2.375$ Å, $d(Ho-O)_{capping}=2.495$ Å, $d(Ho-O)_{mean}=2.413$ Å						
d	2.373 (2.369)	2.523 (2.501)	2.390 (2.380)	2.364 (2.352)	2.484 (2.484)	2.390 (2.382)
σ^2/C_3	$0.0034/1.1\times10^{-5}$	$0.0058/3.2\times10^{-4}$	$0.0076/2.7\times10^{-5}$	$0.0108/6.9\times10^{-5}$	$0.0142/>1.0\times10^{-6}$	$0.0060/1.4\times10^{-5}$
N	6	2.91	8.91	6	2.91	8.91
Ho^{3+}/water (acidic)						
d	2.371 (2.366)	2.501 (2.495)	2.397 (2.385)	2.367 (2.367)	2.502 (2.502)	2.379 (2.379)
σ^2/C_3	$0.0043/1.4\times10^{-5}$	$0.0050/4.0\times10^{-5}$	$0.0078/3.8\times10^{-5}$	$0.0053/>1.0\times10^{-6}$	$0.0068/>1.0\times10^{-6}$	$0.0068/>1.0\times10^{-6}$
N	6	2.91	8.91	6	2.91	8.91
$[Er(H_2O)_9](CF_3SO_3)_3$(s); $d(Er-O)_{prism}=2.355$ Å, $d(Er-O)_{capping}=2.515$ Å, $d(Er-O)_{mean}=2.406$ Å						
d	2.353 (2.345)	2.488 (2.480)	2.372 (2.365)	2.351 (2.343)	2.495 (2.478)	2.365 (2.365)
σ^2/C_3	$0.0061/3.9\times10^{-5}$	$0.0071/3.6\times10^{-5}$	$0.0058/2.2\times10^{-5}$	$0.0044/3.8\times10^{-5}$	$0.0081/1.7\times10^{-5}$	$0.0099/>1.0\times10^{-6}$
N	6	2.95	8.95	6	2.95	8.95
Er^{3+}/water (acidic)						
d				2.355 (2.346)	2.475 (2.465)	2.384 (2.363)
σ^2/C_3				$0.0056/4.1\times10^{-5}$	$0.0080/1.7\times10^{-5}$	$0.0049/1.7\times10^{-5}$
N				6.0	2.95	8.95
$[Tm(H_2O)_9](CF_3SO_3)_3$(s); $d(Tm-O)_{prism}=2.331$ Å, $d(Tm-O)_{capping}=2.513$ Å, $d(Tm-O)_{mean}=2.391$ Å						
d	2.334 (2.330)	2.450 (2.434)	2.356 (2.345)	2.340 (2.330)	2.460 (2.450)	2.350 (2.346)
σ^2/C_3	$0.0042/1.4\times10^{-5}$	$0.0049/3.9\times10^{-5}$	$0.0061/5.2\times10^{-5}$	$0.0086/5.0\times10^{-5}$	$0.0091/4.3\times10^{-5}$	$0.0069/1.6\times10^{-5}$
N	6	2.8	8.8	6	2.8	8.8
Tm^{3+}/water (acidic)						
d				2.349 (2.330)	2.470 (2.453)	2.350 (2.336)
σ^2/C_3				$0.0081/4.2\times10^{-5}$	$0.0073/3.3\times10^{-5}$	$0.0059/6.5\times10^{-5}$
N				6	2.8	8.8
$[Yb(H_2O)_9](CF_3SO_3)_3$(s); $d(Yb-O)_{prism}=2.314$ Å, $d(Yb-O)_{capping}=2.501$ Å, $d(Yb-O)_{mean}=2.376$ Å						
d	2.319 (2.317)	2.460 (2.422)	2.348 (2.339)	2.321 (2.313)	2.430 (2.421)	2.351 (2.338)
σ^2/C_3	$0.0041/0.4\times10^{-5}$ $0.0037/2.7\times10^{-4}$	$0.0098/2.9\times10^{-5}$	$0.0083/1.6\times10^{-5}$	$0.0091/5.3\times10^{-5}$	$0.0102/9.2\times10^{-5}$	
N	6	2.7	8.7	6	2.7	8.7
Yb^{3+}/water (acidic)						
d	2.326 (2.320)	2.443 (2.431)	2.357 (2.345)	2.315 (2.309)	2.430 (2.417)	2.324 (2.324)
σ^2/C_3	$0.0051/1.5\times10^{-5}$	$0.0046/7.5\times10^{-5}$	$0.0092/7.3\times10^{-5}$	$0.0051/2.2\times10^{-5}$	$0.0101/8.2\times10^{-5}$	$0.0049/>1.0\times10^{-6}$
N	6	2.7	8.7	6	2.7	8.7
$[Lu(H_2O)_9](CF_3SO_3)_3$(s); $d(Lu-O)_{prism}=2.296$ Å, $d(Lu-O)_{capping}=2.507$ Å, $d(Lu-O)_{mean}=2.364$ Å						
d	2.304 (2.296)	2.370 (2.360)	2.312 (2.305)	2.318 (2.283)	2.370 (2.370)	2.326 (2.315)
σ^2/C_3	$0.0041/3.0\times10^{-5}$	$0.0029/4.4\times10^{-5}$	$0.0052/1.8\times10^{-5}$	$0.0124/3.9\times10^{-4}$	$0.0105/>1.0\times10^{-6}$	$0.0124/3.1\times10^{-5}$
N	6	2.2	8.2	6	2.2	8.2
Lu^{3+}/water (acidic)						
d	2.293 (2.275)	2.348 (2.342)	2.307 (2.290)	2.282 (2.274)	2.366 (2.343)	2.316 (2.316)
σ^2/C_3	$0.0087/1.5\times10^{-4}$	$0.0043/2.5\times10^{-5}$	$0.0155/1.0\times10^{-4}$	$0.0076/3.5\times10^{-5}$	$0.0081/2.7\times10^{-4}$	$0.0059/>1.0\times10^{-6}$
N	6	2.2	8.2	6	2.2	8.2

ple, the significance when comparing relative shifts in the distances. However, the variations in the refined parameters, including the shift in the E_0 value (for which $k=0$), with different models and data ranges, indicate that the absolute accuracy of the distances given for the separate complexes is within ± 0.01 to 0.02 Å for well-defined interactions. The "standard deviations" given in the text have been increased accordingly to include estimated additional effects of systematic errors.

Acknowledgement

We gratefully acknowledge the financial support from the Swedish Research Council, the European Synchrotron Radiation Facility (ESRF), and the Stanford Synchrotron Radiation Laboratory (SSRL) for allocation of beam time and laboratory facilities. SSRL is operated by the Department of Energy, Office of Basic Energy Sciences. The SSRL Biotechnology Program is supported by the National Institutes of Health, National Center for Research Resources, Biomedical Technology Program, and by the Department of Energy, Office of Biological and Environmental Research. We acknowledge Dr. M. Borowski and the staff at BM29 at ESRF for support.

[1] a) J. K. Marsh, *J. Chem. Soc.* **1939**, *61*, 554–558; b) A. W. Wylie, *R. Aust. Chem. Inst. J. Proc.* **1950**, *17*, 377; c) D. H. Templeton, C. H. Dauben, *J. Am. Chem. Soc.* **1954**, *76*, 5237–5239.
[2] F. H. Spedding, M. J. Pikal, B. O. Ayers, *J. Phys. Chem.* **1966**, *70*, 2440–2449.
[3] F. H. Spedding, K. C. Jones, *J. Phys. Chem.* **1966**, *70*, 2450–2455.
[4] F. H. Spedding, M. J. Pikal, *J. Phys. Chem.* **1966**, *70*, 2430–2440.
[5] T. Yamaguchi, M. Nomura, H. Wakita, H. Ohtaki, *J. Chem. Phys.* **1988**, *89*, 5153–5159.
[6] C. Cossy, A. C. Barnes, J. E. Enderby, *J. Chem. Phys.* **1989**, *90*, 3254–3260.
[7] C. Cossy, L. Helm, D. H. Powell, A. E. Merbach, *New J. Chem.* **1995**, *19*, 27.
[8] C. Cossy, L. Helm, A. E. Merbach, *Inorg. Chem.* **1988**, *27*, 1973–1979.
[9] C. Cossy, L. Helm, A. E. Merbach, *Inorg. Chem.* **1989**, *28*, 2699–2703.
[10] K. Micskei, D. H. Powell, L. Helm, E. Brucher, A. E. Merbach, *Magn. Reson. Chem.* **1993**, *31*, 1011–1020.
[11] D. H. Powell, A. E. Merbach, *Magn. Reson. Chem.* **1994**, *32*, 793.
[12] D. Fay, D. Litchinski, N. Purdie, *J. Phys. Chem.* **1969**, *73*, 544–552.
[13] V. L. Garza, N. Purdie, *J. Phys. Chem.* **1970**, *74*, 275–280.
[14] D. F. Peppard, G. W. Mason, S. Lewey, *J. Inorg. Nucl. Chem.* **1969**, *31*, 2271–2272.
[15] a) G. Schwarzenbach, R. Gut, G. Anderegg, *Helv. Chim. Acta* **1954**, *37*, 937–957; b) E. Wheelwright, F. H. Spedding, G. Schwarzenbach, *J. Am. Chem. Soc.* **1953**, *75*, 4196–4201.
[16] D. F. Peppard, C. A. A. Bloomquist, E. P. Horwitz, S. Lewey, G. W. Mason, *J. Inorg. Nucl. Chem.* **1970**, *32*, 339–343.
[17] S.-I. Ishiguro, R. Kato, R. Takahashi, S. Nakasone, *Rare Earths Mod. Sci. Technol.* **1995**, *27*, 61–77.
[18] J. A. Solera, J. García, M. G. Proietti, *Phys. Rev. B* **1995**, *208*, 2678–2686.
[19] J. M. B Harrowfield, D. L. Kepert, J. M. Patrick, A. H. White, *Aust. J. Chem.* **1983**, *36*, 483–492.
[20] A. Chatterjee, E. N. Maslen, K. J. Watson, *Acta Crystallogr. Sect. B* **1988**, *44*, 381–386.
[21] C. O. P. Santos, E. E. Castellano, L. C. Machado, G. Vicentini, *Inorg. Chim. Acta* **1985**, *110*, 83–86.
[22] A. Chatterjee, *Pak. J. Sci. Ind. Res.* **1986**, *29*, 381.
[23] A. Abbasi, P. Lindqvist-Reis, L. Eriksson, D. Sandström, S. Lidin, I. Persson, M. Sandström, *Chem. Eur. J.* **2005**, *11*, 4065–4077.
[24] J. Albertsson, I. Elding, *Acta Crystallogr. Sect. B* **1977**, *33*, 1460–1469.
[25] R. E. Gerkin, W. J. Reppart, *Acta Crystallogr. Sect. C* **1984**, *40*, 781–786.
[26] C. R. Hubbard, C. O. Quicksall, R. A. Jacobson, *Acta Crystallogr. Sect. B* **1974**, *30*, 2613–2619.
[27] J. Albertsson, I. Elding, *Acta Crystallogr. Sect. B* **1977**, *33*, 1460–1469.
[28] S. K. Sikka, *Acta Crystallogr. Sect. A* **1969**, *25*, 621–626.
[29] J. C. Gallucci, R. E. Gerkin, W. J. Reppart, *Cryst. Struct. Commun.* **1982**, *11*, 1141–1145.
[30] R. E. Gerkin, W. J. Reppart, *Acta Crystallogr. Sect. C* **1987**, *43*, 623–631.
[31] D. R. Fitzwater, R. E. Rundle, *Z. Kristallogr. Kristallgeom. Kristallphys. Krista* **1959**, *112*, 363.
[32] K. C. Lim, B. W. Skelton, A. H. White, *Aust. J. Chem.* **2000**, *53*, 867–873.
[33] T. Timofeeva, A. Babai, G. Meyer, A.-V. Mudring, *Acta Crystallogr. Sect. E* **2005**, *61*, i94-i95.
[34] T. Timofeeva, A. Babai, G. Meyer, A.-V. Mudring, *Acta Crystallogr. Sect. E* **2005**, *61*, i87-i88.
[35] P. C. Junk, L. I. Semenova, B. W. Skelton, A. H. White, *Aust. J. Chem.* **1999**, *52*, 531–538.
[36] P. Lindqvist-Reis, K. Lamble, S. Pattanaik, M. Sandström, I. Persson, *J. Phys. Chem. B* **2000**, *104*, 402–408.
[37] P. Lindqvist-Reis, I. Persson, M. Sandström, *Dalton Trans.* **2006**, 3868–3878.
[38] I. Persson, P. Persson, M. Sandström, A.-S. Ullström, *J. Chem. Soc. Dalton Trans.* **2002**, 1256–1265.
[39] G. M. Sheldrick, SHELXS97 and SHELXL97, Computer program for the solution and refinement of crystal structures, Göttingen, Germany, **1997**.
[40] G. Bergerhoff, DIAMOND—Visual Crystal Structure Information System, Bonn, Germany, **1996**.
[41] A. L. Spek, *J. Appl. Crystallogr.* **2004**, *37*, 7–13.
[42] A. Filipponi, M. Borowski, D. T. Bowron, S. Ansell, A. Di Cicco, S. De Panfilis, J.-P. Itiè, *Rev. Sci. Instrum.* **2000**, *71*, 2422–2432.
[43] A. Kodre, I. Arčon, M. Hribar, M. Stuhec, F. Villain, W. Drube, L, Tröger, *Phys. Rev.* B **1995**, *208*, 379–380.
[44] P. D'Angelo, S. De Panfilis, A. Filipponi, I. Persson, *Chem. Eur. J.* **2008**, *14*, DOI:10.102/chem.200701282.
[45] R. D. Shannon, *Acta Crystallogr. Sect. A* **1976**, *32*, 751–767.
[46] J. K. Beattie, S. P. Best, B. W. Skelton, A. H. White, *J. Chem. Soc. Dalton Trans.*, **1981**, 2105–2111.
[47] S. Kobayashi, *Eur. J. Org. Chem.* **1999**, 15–27.
[48] C. F. Baes, R. E. Mesmer, *The Hydrolysis of Cations*, Krieger Publishing Company, Malabar, FL, **1986**, Chap. 7, and references therein.
[49] Oxford Diffraction Ltd., Xcalibur CCD system, CrysAlis Software system, Version 1.17, **2003**.
[50] A. Thompson, D. Attwood, E. Gullikson, M. Howells, K.-J. Kim, J. Kirz, J. Kortright, I. Lindau, P. Pianatta, A. Robinson, J. Scofield, J. Underwood, D. Vaughan, G. Williams, H. Winick, *X-ray Data Booklet*, LBNL/PUB-490 Rev. 2, Lawrence Berkeley National Laboratory, Berkeley, CA, **2001**.
[51] G. N. George, I. J. Pickering, EXAFSPAK—A Suite of Computer Programs for Analysis of X-Ray Absorption Spectra, SSRL, Stanford, CA, **1993**.
[52] A. Filipponi, A. Di Cicco, C. R. Natoli, *Phys. Rev. B* 1995, **52**, 15122–15134.
[53] A. Filipponi, A. Di Cicco, *Phys. Rev. B* **1995**, *52*, 15135–15149.
[54] A. Filipponi, *J. Phys. Condens. Matter* **1994**, *6*, 8415–8427.
[55] L. Hedin, B. I. Lundqvist, *J. Phys. C.* **1971**, *4*, 2064–2083.

Received: August 7, 2007
Published online: February 18, 2008

